High-precision mass measurements of the isomeric and ground states of ^{44}V: Improving constraints on the isobaric multiplet mass equation parameters of the $A = 44$, 0^+ quintet

D. Puentes [1,2,*] G. Bollen,[1,3] M. Brodeur,[4] M. Eibach,[5] K. Gulyuz,[6] A. Hamaker [1,2] C. Izzo,[1,2,†] S. M. Lenzi,[7,8]
M. MacCormick,[9] M. Redshaw [2,6] R. Ringle,[2] R. Sandler,[2,6] S. Schwarz,[2] P. Schury,[10] N. A. Smirnova,[11] J. Surbrook,[1,2]
A. A. Valverde [4,‡] A. C. C. Villari,[3] and I. T. Yandow[1,2]

[1]*Department of Physics and Astronomy, Michigan State University, East Lansing, Michigan 48824, USA*
[2]*National Superconducting Cyclotron Laboratory, East Lansing, Michigan 48824, USA*
[3]*Facility for Rare Isotope Beams, East Lansing, Michigan 48824, USA*
[4]*Department of Physics, University of Notre Dame, Notre Dame, Indiana 49556, USA*
[5]*Institut für Physik, Ernst-Moritz-Arndt-Universität, 17487 Greifswald, Germany*
[6]*Department of Physics, Central Michigan University, Mount Pleasant, Michigan 48859, USA*
[7]*Dipartimento di Fisica e Astronomia "Galileo Galilei", Universitá di Padova, I-135131 Padova, Italy*
[8]*INFN, Sezione di Padova, I-35131 Padova, Italy*
[9]*Université Paris-Saclay, CNRS/IN2P3, IJCLab, 91405 Orsay, France*
[10]*Wako Nuclear Science Center (WNSC), Institute of Particle and Nuclear Studies (IPNS), High Energy Accelerator Research Organization
(KEK), Wako, Saitama 351-0198, Japan*
[11]*CENBG, CNRS/IN2P3 and Université de Bordeaux, Chemin du Solarium, 33175 Gradignan Cedex, France*

Background: The quadratic isobaric multiplet mass equation (IMME) has been very successful at predicting the masses of isobaric analog states in the same multiplet, while its coefficients are known to follow specific trends as functions of mass number. The Atomic Mass Evaluation 2016 [Chin. Phys. C **41**, 030003 (2017)] ^{44}V mass value results in an anomalous negative c coefficient for the IMME quadratic term; a consequence of large uncertainty and an unresolved isomeric state. The b and c coefficients can provide useful constraints for construction of the isospin-nonconserving Hamiltonians for the pf shell. In addition, the excitation energy of the 0^+, $T = 2$ level in ^{44}V is currently unknown. This state can be used to constrain the mass of the more exotic ^{44}Cr.

Purpose: The aim of the experimental campaign was to perform high-precision mass measurements to resolve the difference between ^{44}V isomeric and ground states, to test the IMME using the new ground state mass value and to provide necessary ingredients for the future identification of the 0^+, $T = 2$ state in ^{44}V.

Method: High-precision Penning trap mass spectrometry was performed at LEBIT, located at the National Superconducting Cyclotron Laboratory, to measure the cyclotron frequency ratios of $[^{44g,m}VO]^+$ versus $[^{32}SCO]^+$, a well-known reference mass, to extract both the isomeric and ground state masses of ^{44}V.

Results: The mass excess of the ground and isomeric states in ^{44}V were measured to be $-23\,804.9(80)$ keV/c^2 and $-23\,537.0(55)$ keV/c^2, respectively. This yielded a new proton separation energy of $S_p = 1\,773(10)$ keV.

Conclusion: The new values of the ground state and isomeric state masses of ^{44}V have been used to deduce the IMME b and c coefficients of the lowest 2^+ and 6^+ triplets in $A = 44$. The 2^+ c coefficient is now verified with the IMME trend for lowest multiplets and is in good agreement with the shell-model predictions using charge-dependent Hamiltonians. The mirror energy differences were determined between ^{44}V and ^{44}Sc, in line with isospin-symmetry for this multiplet. The new value of the proton separation energy determined, to an uncertainty of 10 keV, will be important for the determination of the 0^+, $T = 2$ state in ^{44}V and, consequently, for prediction of the mass excess of ^{44}Cr.

I. INTRODUCTION

Isospin is a quantum number that was postulated by Heisenberg after the discovery of the neutron [1] to explain symmetries between the new nucleon and the proton [2]. In this formalism a nucleon is assumed to carry an isospin quantum number $t = 1/2$, similar to an ordinary spin, with proton and neutron being labeled by its projection $t_z = \pm1/2$. Therefore, the three components of the isospin operator, $\hat{t}$, obey

---
*puentes@nscl.msu.edu
†Current address: TRIUMF, 4004 Wesbrook Mall, Vancouver, British Columbia, Canada V6T 2A3.
‡Current address: Physics Division, Argonne National Laboratory, Lemont, Illinois 60439, USA.

well-known SU(2) commutation relations: $[\hat{t}_j, \hat{t}_k] = i\epsilon_{jkl}\hat{t}_l$. The total isospin operator for an A-nucleon system is $\hat{T} = \sum_{n=1}^{A} \hat{t}(n)$, while its projection is $\hat{T}_z = \sum_{n=1}^{A} \hat{t}_z(n)$. A charge-independent Hamiltonian would commute with isospin operator, $[\hat{H}, \hat{T}] = 0$, giving rise to degenerate multiplets of states (J^π, T) in nuclei with the same A and $T_z = -T, \ldots, T$, called *isobaric analog states (IAS)*.

However, the Coulomb interaction between protons, the proton-neutron mass difference, and small charge-dependent components in phenomenological nuclear interactions lead to an energy splitting of the isobaric multiplet states. Wigner showed [3] that, assuming a two-body nature of charge-dependent forces, the splitting of the isobaric multiplets follows the quadratic dependence as a function of T_z, establishing what is known as the isobaric multiplet mass equation (IMME):

$$\text{M.E.}(\alpha, T) = a(\alpha, T) + b(\alpha, T)T_z + c(\alpha, T)T_z^2, \quad (1)$$

where α denotes all other relevant quantum numbers which characterize a given multiplet $(A, J, \pi, \ldots)$.

The quadratic IMME describes well the energy splittings of the isobaric multiplet states [3]. For quartets and quintets, it is often used to determine masses of unknown members belonging to the same multiplet. Data from high-precision mass measurements and other experimental techniques have made it possible to work out extensive compilations of the experimental a, b, and c coefficients for the lowest and higher lying multiplets up to about $A = 71$ (the most recent evaluations can be found in Refs. [4,5]). Some intriguing results are unveiled from the behavior of the IMME coefficients as a function of A, which manifests in specific trends and even characteristic fine structure (staggering) for $T = 1/2, 1, 3/2$. In addition, any manifestation of a deviation from a quadratic IMME in quartets or quintets is also of high interest since it could either be related to isospin mixing or bring important information on the presence of charge-dependent many-body forces [6–8].

Understanding the a, b, and c coefficients is important for nuclear structure theory, since they serve as a probe of the strengths of the isoscalar, isovector and isotensor components of the nuclear force, respectively, and therefore can shed light onto the magnitude of the charge-dependent terms of the effective nucleon-nucleon interaction in different approaches [9–16]. While the main contribution comes from the Coulomb interaction between the charged protons, the charge-dependent components of nuclear origin are not negligible and have to be taken into account for a realistic description.

A precise description of the IMME coefficients remains challenging for nuclear theory and numerous studies are underway. For lighter, sd and pf shell, nuclei the most accurate predictions are due to the shell-model with phenomenological isospin-nonconserving (INC) Hamiltonians [10,15]. To construct such a Hamiltonian, one adds to a well-established isospin-conserving Hamiltonian, such as USD [17,18] in the sd shell, a charge-dependent part, consisting of the two-body Coulomb interaction, an isovector and an isotensor term describing effective charge-dependent two-body forces of nuclear origin, and isovector single-particle energies. The

strengths of those terms are adjusted to match the experimentally extracted IMME b and c coefficients. For the sd shell this task was accomplished in the 1990s [10,11] and recently updated [15], using a more extensive database. There has been less progress with the pf shell, however. In Ref. [10], while the isovector strength parameter in the pf shell was obtained by a fit of the b coefficients, the strength of the isovector component of nuclear origin was estimated to be approximately 4% of the $T = 1$ two-body matrix elements. One reason for that is the difficulty of the calculations at that time, while the other reason was the lack of experimental data.

Modern progress in the shell-model computations gave rise to new higher precision effective interactions for large-scale calculations in the full pf shell, such as GXPF1A [19] or KB3G [20]. The INC version of GXPF1A, which we call here cdGX1A, still adapts the charge-dependent terms parametrization from Refs. [10,21]. The recently derived microscopic INC pf shell Hamiltonians [22], based on the modern NN potentials and many-body perturbation theory, show themselves to be less successful than earlier phenomenological parametrizations. It would be interesting to further test the predictions of phenomenological INC interactions on an updated experimental database, and, if necessary, to work out a well-adjusted pf shell INC interaction.

A high-precision INC Hamiltonian would provide a framework to understand the structure and decay modes of proton rich nuclei, including mass predictions for nuclei in the vicinity of the proton drip-line. This would have consequences for nuclear astrophysics (e.g., for the rp process). Another important application of such interactions is the calculation of nuclear structure corrections to superallowed Fermi β decay between isobaric analog states, used for the tests of the CVC hypothesis and the CKM matrix unitarity tests [21,23,24].

A full analysis of IMME coefficients for the ground state of nuclei completed for $T = 1/2$ to 3 multiplets was performed [5] using the Atomic Mass Evaluation (AME) 2012 and the Evaluated Nuclear Structure Data Files [25,26]. There were different cases where unknown mass values were the largest source of uncertainty. For the $T = 1$ triplet at $A = 44$, the measured ground state of ^{44}V produced an improbable negative c coefficient in the IMME. At the same time, the predicted value from the c coefficient systematics was around 145 keV [5]. If it were true, it would point to the possibility of new physics. With such a large uncertainty, new high-precision measurements are necessary to resolve the discrepancy in the c coefficient and determine how well the INC-Hamiltonian describes the $A = 44$ case. This creates an anchor for the $A = 4n$ nuclei (where n is an integer) and provides the information necessary to formulate a complete $sdpf$ shell model description of light nuclei.

In the last two decades, significant progress has been made in understanding the Coulomb energy shifts in isobaric analog states for both mirror energy differences (MEDs) and triplet energy differences (TEDs). These quantities for doublets and triplets are related to the differences in the b and c coefficients of the excited and lowest multiplets: $\text{MED}_J = -2\Delta b_J$, $\text{TED}_J = 2\Delta c_J$ (the latter is not defined for $T = 1/2$ doublets). The theoretical description of MEDs and TEDs in the pf shell using an INC Hamiltonian for the pf shell has been a
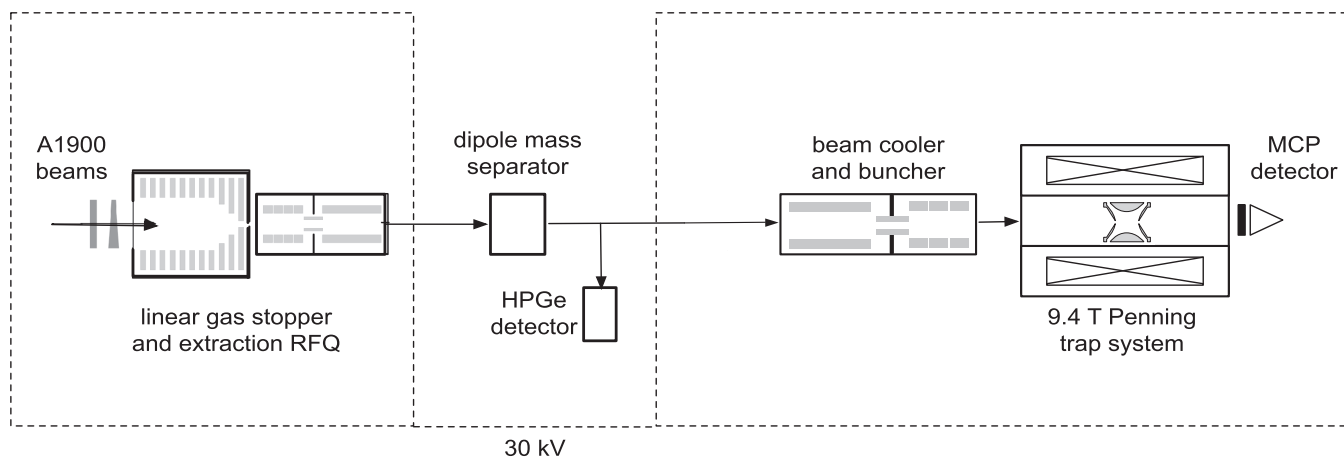
FIG. 1. Schematic diagram of the experimental setup including the beam stopping area, low energy transport/mass separation, LEBIT cooler/buncher, and 9.4 T Penning Trap system.

great success [12]. A particular feature of the approach is the use of an effective two-body component, of nuclear origin, parametrized in the form of a few specific two-body matrix elements. For the pf shell, there was evidence that an additional isovector two-body matrix element for the $f_{7/2}$ subshell in the MED was needed. In the TED, there is evidence that an additional isotensor two-body matrix element is necessary for the $f_{7/2}$ subshell. There was also a study of ^{44}V showing that the $J = 2$ matrix elements differ from the other $T = 1$ multiplets as described by theory [27]. Application of that description to the $A = 44$ case was difficult since the position of the 6^+ isomer was not known. The high-precision measurement of the 6^+ ^{44}V isomeric state provides experimental constraints on both the MED and TED studies in this region [27].

Due to a lack of experimental data for the ^{44}Cr nucleus, the 0^+ quintet group in $A = 44$ is even less well known [28]. Precise knowledge of the ^{44}V mass is required for an accurate determination of the mass excess of the 0^+, $T = 2$ state, an IAS of the ^{44}Cr ground state. This will provide the first experimental constraint on the ground-state binding energy of ^{44}Cr. The β-delayed proton decay of ^{44}Cr has been observed experimentally [29,30], but the assignment of the proton branch from the IAS was tentative. A more precise value of the one-proton separation energy in ^{44}V will contribute to future studies aimed at identifying the exact location of the proton-emitting level, to establish whether it is from the IAS or not, and will also be useful in pinning down the positions of other proton-unbound levels.

Recently, a mass measurement of ^{44}V was performed using isochronous mass spectrometry at the Cooler Storage Ring (CSRe), Lanzhou [31]. They were able to resolve the ground and isomeric state of ^{44}V, and found a new c coefficient that agreed with the predicted IMME parameters. Through a high-precision measurement using Penning trap mass spectrometry, we are in a position to verify their mass measurements, which currently disagrees by 1.7σ with the AME2016 [28] for the ground state and 1.7σ for the isomeric state using the prediction from [27] with the AME2016 value.

II. EXPERIMENTAL METHODS

At the National Superconducting Cyclotron Laboratory (NSCL), a radioactive ^{44}V beam was produced through projectile fragmentation. A stable ^{58}Ni beam was accelerated using the Coupled Cyclotron Facility (CCF) to an energy of 160 MeV/nucleon, and impinged on a ^{9}Be target with a thickness of 705 mg/cm^2. After the target station, the cocktail beam was purified in the A1900 Fragment Separator [32].

The beam energy was degraded in a 1530 μm thick Al plate and a 1050 μm thick glass silica wedge to $\approx$1 MeV/nucleon [32]. The beam was then delivered to a gas cell, filled with high purity He buffer gas at a pressure of 71 mbar, to stop the radioactive beam [33]. The ions were extracted through a radiofrequency quadrupole (RFQ), accelerated to an energy of 30 keV, and purified using a magnetic dipole mass separator based on the mass to charge ratio (A/Q). The resolving power of the mass separator is $\approx$1500. The thermalized beam showed the most activity at $A/Q = 60$, corresponding to $[^{44}$VO$]^+$ molecular ion.

The low-energy beam was then guided through an electrostatic beam transport system to the Low Energy Beam and Ion Trap (LEBIT) experimental station [34], as shown in Fig. 1. The first component of the LEBIT station is a two-stage cooler and buncher [35]. The cooler stage uses He buffer gas to continue thermalizing the beam while the buncher converts the DC beam into a pulsed beam. The ions are then ejected into the 9.4 T Penning trap. Once trapped, the ions were first purified using narrow-band and SWIFT rf dipole excitations [36,37] via segmented ring electrodes on the trap to remove contaminant ions. The time-of-flight ion cyclotron resonance (TOF-ICR) technique was used to measure the cyclotron frequency, $\nu_c = qB/(2\pi \cdot m)$, of an ion of interest of mass m and charge q in a magnetic field B [38,39]. A TOF response curve is shown in Fig. 2, where both the isomer and ground state are resolved. The data were fitted with a theoretical line shape from which the cyclotron frequency was extracted [39]. All measurements of $[^{44}$VO$]^+$ were performed
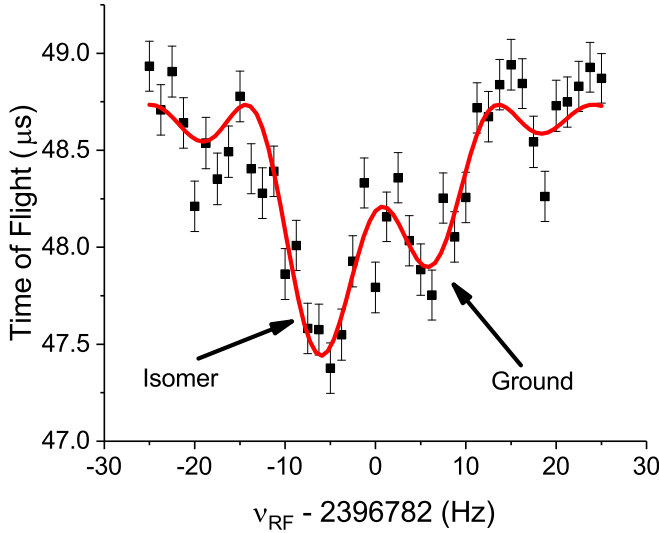
FIG. 2. A 100-ms $[^{44}VO]^+$ time-of-flight cyclotron double reso-nance used for determining the ν_c of $[^{44}VO]^+$. The line shape is a theoretical curve described in [39]. Both the isomer and the ground state of ^{44}V are visible.

using a 100 ms excitation time, whereas the reference ion $([^{32}SCO]^+)$ was measured using a 500 ms excitation time.

III. RESULTS

The frequency ratio of the ion of interest ν_c to the reference ion $\nu_{c,ref}$, $\bar{R} = \nu_c/\nu_{c,ref}$, is used to determine the mass of the ion of interest. This ratio is obtained by alternating measure-ments of the reference ion and the ion of interest. Whenever the cyclotron frequency of $[^{44}VO]^+$ was measured, there was also an associated measurement of the cyclotron frequency of the reference ion, $[^{32}SCO]^+$, taken before and after. The refer-ence ion was measured with a longer excitation time to ensure that the uncertainty in the frequency of the reference ion does not contribute significantly to the uncertainty of the ratio. These two reference measurements are used to interpolate the value of B at the time $[^{44}VO]^+$ was measured. In this manner a ratio of the frequency of interest to the frequency of the well-known reference ion is determined. After repeating this cycle multiple times the mean frequency ratio $\bar{R}$ is obtained.

Measurements were taken over an 80-h period. Due to low statistics, multiple measurements were compiled into five combined resonance curves. The mean frequency ratio for the ground state of $[^{44}VO]^+$ vs $[^{32}SCO]^+$ was measured to be $\bar{R} = 0.999\,960\,43(13)$ with a Birge ratio [40] of 1.07(21). The mean frequency ratio for the isomeric state was measured to be $\bar{R} = 0.999\,955\,631(75)$ with a Birge ratio of 1.31(21).

Since the Birge ratios were greater than 1, the uncertainties of $\bar{R}$ were inflated to account for potential systematic uncertain-ties.

The mass excess of ^{44}V was extracted using

$$m_V = \frac{1}{\bar{R}}(m_S - m_e) + m_e, \qquad (2)$$

where m_V is the mass of $[^{44}VO]$, m_S is the mass of $[^{32}SCO]$, and m_e is the mass of the electron. m_S is determined from the AME2016 mass values of its constituent isotopes [28]. The molecular binding energy and ionization energy of the singly charged molecular ion are on the order of eV or less and are not included.

The measured effect from previous work of nonlin-ear magnetic field fluctuations was on the order of 3.0×10^{-10} hour [41]. The longest measurement, after combining measurements due to low statistics, was 12 h. However, since the reference ion and ion of interest are similar in mass, the effect of magnetic field fluctuations is negligible. A large number of ions in the trap can lead to frequency shifts due to the Coulomb interaction between the trapped ions. When measurements are performed with many ions in the trap (e.g., five or more), a count (z) class analysis [42] is used to extrapolate the frequency of a single ion in the trap. Data are analyzed based on the number of ions in the trap (a count class), followed by a fit of each class to determine a frequency. The frequency of a single ion in the trap is then extrapolated from a linear regression of this data. A count class analysis was not necessary due to the low statistics of the experiment because events with only five ions or fewer were used for the analysis. Finally, due to the similarity in mass between the reference ion and ion of interest, relativistic effects did not need to be considered.

The results of the data analysis are shown in Table I. These values agree with the values reported in [31], but are a factor of 2–4 more precise. Our new mass values also disagree with the AME2016 by 1.6σ for the ground state and by 1.7σ for the isomeric state. The AME2016 value was adopted from the AME2012 value, which was evaluated from [43]. The ^{44}V mass excess was determined by using experimental fit parameters obtained during the experimental ring storage experiment reported by [43]. A new proton separation energy for ^{44}V is determined to be $1\,773(10)$ keV.

IV. DISCUSSION

Previous work from [27] established a level scheme based on measured γ rays. However, as the energy of the iso-meric state was unknown, many excited state energies of ^{44}V were determined relative to the isomeric state. Using

TABLE I. Mean frequency ratios, $\bar{R} = \nu_c/\nu_{c,ref}$, calculated atomic mass and mass excess (ME) values, and their comparison to the values from Ref. [31]. The uncertainty reported in curly brackets for the $\bar{R}$ are the inflated uncertainties after taking into account the Birge ratio.

Isotope	Measured ion	Reference	$\bar{R}$	Mass (^{44}V) (u)	ME (^{44}V) (keV)	Ref. [31] (keV)
^{44}V	$^{44}VO^+$	$[^{32}SCO]^+$	0.999 960 43(13){14}	43.974 444 1(84)	−23 804.9(80)	−23 827(20)
^{44m}V	$^{44m}VO^+$	$[^{32}SCO]^+$	0.999 955 631(75){98}	43.974 731 9(57)	−23 537.0(55)	−23 541(19)

TABLE II. Newly constrained levels of ^{44}V based on the resolved isomeric state. This work shows the experimental data while [27] is based on shell-model calculations, with the only uncertainty coming from the γ rays observed in Ref. [27].

J^π	This work + Ref. [27] (keV)	Ref. [27] (keV)
(7^+)	981.7(98)	979.9(5)
(9^+)	2 661.7(99)	2 659.9(17)
(10^+)	4 027(10)	4 024.9(19)
(11^+)	3 494(10)	3 491.9(18)

our new measurement reported here, the excitation energies were experimentally determined with uncertainties based on the energy uncertainty of the isomeric state. Values for the ^{44}V excited state energies are listed in Table II compared to predictions from shell model calculations. These values were used to calculate the experimental MEDs and TEDs, which are explained in further detail in Sec. IV B.

A. IMME b and c coefficients of the lowest $A = 44$, $T = 1$ multiplets

The new values of the mass excesses of ^{44}V and ^{44m}V complete the set of experimental data for the lowest 2^+ and 6^+, $T = 1$ multiplets in $A = 44$ and enable the deduction of new values of their respective IMME b and c coefficients using Eq. (1). The b coefficient for the 2^+, $T = 1$ triplet is deduced to be $b = -7005.5(41)$ keV, while the new value for its c coefficient is 131.75(420) keV. As seen from Fig. 3, which depicts IMME b and c coefficients for the lowest pf shell triplets, both values for $A = 44$ match well the known systematics in this mass region. This resolves the anomaly previously existing at $A = 44$ and verifies the work performed by [31]. The experimental b and c coefficients for the lowest 6^+ triplet have values $-7003.9(2.7)$ keV and 158.9(2.8) keV, respectively.

To understand these values and to test the existing theoretical models, we performed shell-model calculations in the full pf shell using NuShellX@MSU [45] code with two different charge-dependent Hamiltonians, cdGX1A and cdFPD6. These Hamiltonians are based on the isospin-conserving Hamiltonians, GXPF1A [19] and FPD6 [46], respectively, to which have been added the two-body Coulomb interaction, effective nuclear charge-symmetry breaking and charge-independence breaking terms from Ref. [10], and isovector single-particle energies from Ref. [21]. These interactions can be found in the NuShellX@MSU package. A scaling factor proportional to $\sqrt{\hbar\omega(A)}$ is imposed on the Coulomb interaction and isovector single-particle energies to account for the mass-dependence throughout the shell.

Theoretical values of the IMME b and c coefficients for the lowest 2^+ and 6^+ multiplets in $A = 44$, as obtained with cdGX1A and cdFPD6, are given in Table III. Regarding c coefficients, there is a remarkable agreement of theory with the data, especially for the 2^+ multiplet. For b coefficients, we observe more discrepancy between theory and experiment, of the order of 20–30 keV. This is roughly the average precision currently reached for the pf shell. To demonstrate, we show
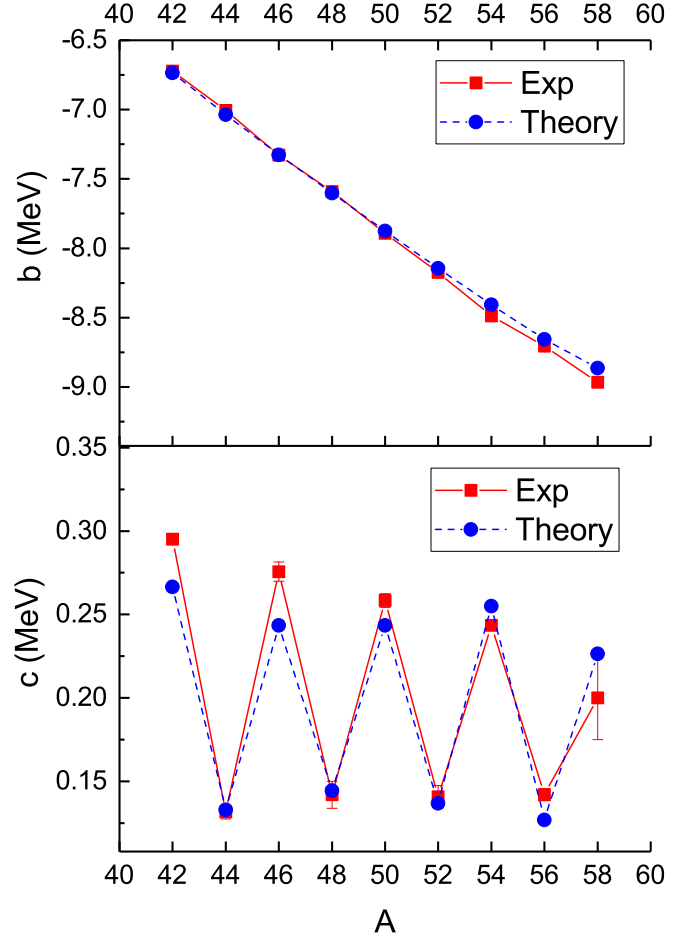

FIG. 3. Experimental (square) and theoretical (circle) b and c coefficients of the lowest triplets in the pf shell, as a function of mass number A. The experimental information came from references [28–30,44] and this work on $A = 44$ ground state mass measurements. Theoretical calculations have been performed with cdGX1A Hamiltonian [45].

in Fig. 3 the cdGX1A predictions for the IMME b and c in the pf shell from $A = 42$ to $A = 58$. The root-mean-square deviation for b coefficients is 48 keV, for c coefficients is 17 keV. We conclude that there is very good agreement of the current phenomenological description with experiment.

The isomeric 6^+ state in ^{44}V is found by cdGX1A to be the first excited state at 282 keV (cdGX1A) above the 2^+ ground state. cdFPD6 is less predictive: the 6^+ state is

TABLE III. New experimental and theoretical IMME b and c coefficients for the lowest 2^+ and 6^+ triplets in $A = 44$.

$A = 44$	2^+		6^+	
	b keV	c keV	b keV	c keV
Exp	$-7\,005.5(41)$	132(5)	$-7\,003.9(27)$	159(3)
cdGX1A	$-7\,035$	133	$-7\,025$	153
cdFPD6	$-7\,037$	132	$-7\,019$	146

TABLE IV. A comparison of the experimental MED for the $T = 1$, $J = 6$ isomeric state in ^{44}V-^{44}Sc mirror nuclei with the theoretical value obtained using Eq. (4).

Parameter	Value
Experimental MED (keV)	−3(10)
Theoretical MED (keV)	−3.3
V_{CM} (keV)	−26
V_B (keV)	−1.3
V_{Cm} (keV)	+24

found to be the second cdGX1A excited state at 643 keV (cdFPD6) above the 2^+ ground state, with the 4^+ state being slightly below. As seen from Table III, the calculated values of the b and c coefficients using either Hamiltonian are in fair agreement with the experimental value. In spite of these already encouraging results, it will definitely be beneficial in future construction of the INC interactions of improved precision to take into account the $A = 44$ data on b and c coefficients.

B. Mirror and triplet energy difference

Differences between the excitation energy of analog states in mirror nuclei, MEDs, can now be deduced and compared with the shell-model calculations using INC interactions:

$$\text{MED(J)} = E^*_{T_z=-1}(J) - E^*_{T_z=+1}(J). \quad (3)$$

Following Refs. [12,47], we consider the contribution of three charge-dependent terms: the multipole Coulomb term that results from the expectation value of the Coulomb potential in both nuclei at each value of J [$V_{CM}(J)$], and other two terms of monopole origin [$V_{Cm}(J)$]. The first one is related to the change of the nuclear radius as a function of the spin and the second is related to corrections to the single-particle energies of protons and neutrons [12]. Systematic studies of nuclei in the $f_{7/2}$ shell have shown the need of adding an isospin-symmetry breaking term [$V_B(J)$] originally deduced from the experimental MED values (^{42}Ti-^{42}Ca) for two protons and two neutrons in the $f_{7/2}$ shell [48], and later extended to all active orbits [49,50]. It consists of an isovector correction to the matrix element for two nucleons coupled to $J = 0$, $T = 1$ with a strength of 100 keV smaller for protons than for neutrons. In this work we have taken into account the four orbits of the pf shell. Theoretical calculations were performed using the GXPF1A effective interactions in the full pf shell.

The MED are calculated through the summation of all the potential contributions (Δ_M stands for the difference between the mirror states):

$$\text{MED(J)} = \Delta_M V_{CM}(J) + \Delta_M V_{Cm}(J) + \Delta_M V_B(J). \quad (4)$$

Table IV summarizes the experimental MED for the 6^+ state in comparison to the MED obtained using Eq. (4). The results show that the contribution from the V_B term is negligible and, interestingly, the small MED results from the mutual cancellation of the monopole (V_{Cm}) and multipole Coulomb (V_{CM}) terms. The increase of the monopole contribution with spin is

interpreted as a shrinking of the radius with increasing angular momentum. This can be deduced from the shell model wave functions looking at the dramatic decrease of the occupation of the p orbits, that have larger radius than the f orbits in the pf shell, as explained in [12,47]. On the other hand, the decrease of the multipole contribution is due to the reduction of Coulomb repulsion through the alignment of protons in ^{44}V at $J = 6$. These two effects are of the same magnitude but of opposite sign, and cancel out at the isomeric state.

This analysis can be extended to other yrast excited states reported in Ref. [27]. Yrast states are the lowest-energy states for given angular momentum [51]. Together with the triplet energy differences, TEDs, among the $T = 1$ isobaric analog states in ^{44}V, ^{44}Sc, and ^{44}Ti:

$$\text{TED(J)} = E^*_{T_z=-1}(J) + E^*_{T_z=+1}(J) - 2E^*_{T_z=0}(J). \quad (5)$$

Theoretically, these are obtained following [12,48]:

$$\text{TED}(J) = \Delta_T V_{CM}(J) + \Delta_T V_B(J), \quad (6)$$
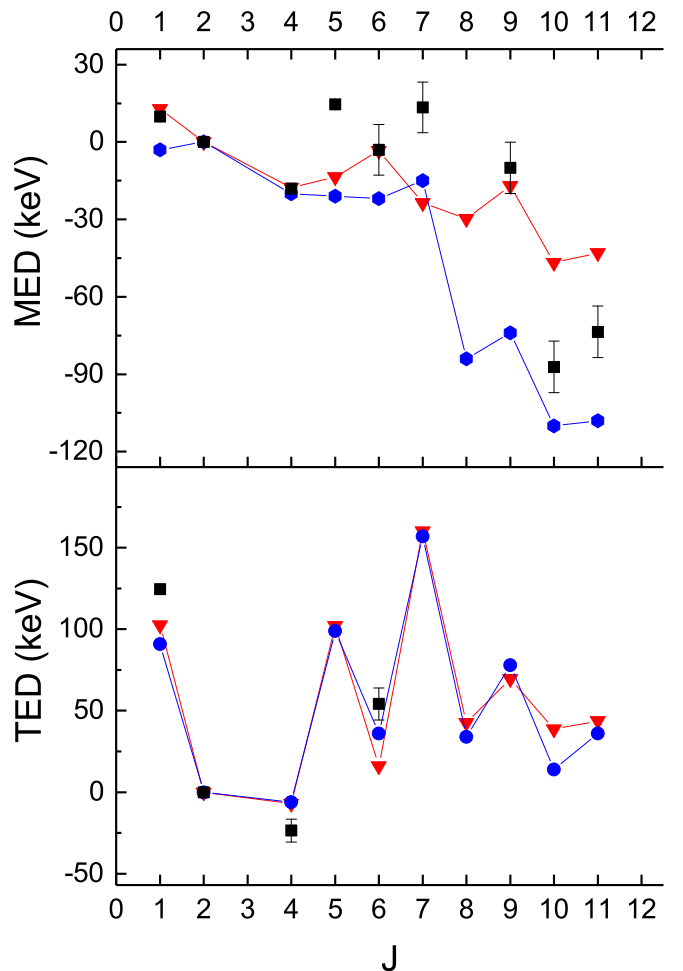

FIG. 4. Mirror and triplet energy differences as a function of J for $A = 44$. Experimental values (square) are compared with those obtained with two different shell model calculations: (circle) with the cdGX1A effective interaction [45] and (triangle) using Eqs. (4), (6) [12]. See text for details.
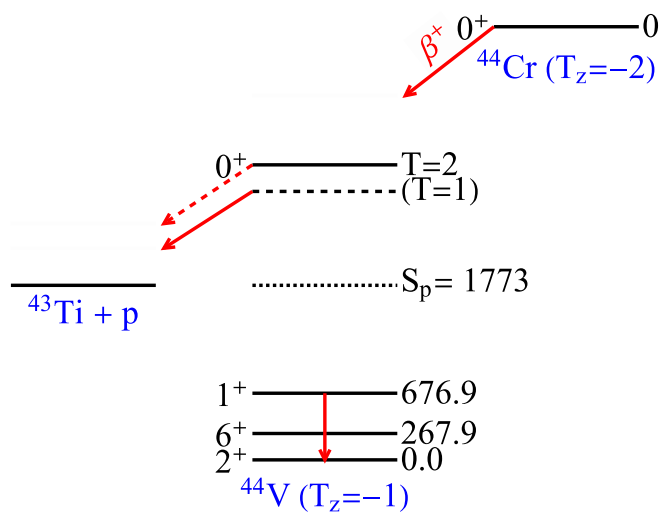
FIG. 5. Experimental partial decay scheme of ^{44}Cr, including new results calculated with the new precise mass measurements of the ground and isomeric states of ^{44}V. The experimental information came from Refs. [28–30]. The level denoted $(T = 1)$ refers to the unknown $J = 1^+$, $T = 1$ state (or states) that can undergo proton emission, in the vicinity of the IAS. The red dashed transition represents the isospin-forbidden transition to ^{43}Ti.

where Δ_T indicates the difference between the triplet states as in Eq. (5). We note that in the TED the monopole contributions cancel out by construction. The V_B term consists of an isotensor correction to the matrix element for two nucleons coupled to $J = 0, T = 1$ with a strength of 100 keV. MED and TED experimental values for the yrast states in $A = 44$ are shown in Fig. 4. They are compared to the calculations using Eqs. (4) and (6), respectively, and with the cdGX1A interaction. Both theoretical results are in fairly good agreement with data. For the MED, the difference between both theoretical approaches reside mainly in the monopole correction. These differences disappear in the TED where both methods give similar predictions.

C. Constraints for the ground state mass of ^{44}Cr

A new mass excess value of the ground state of ^{44}V provides a definitive value for a one-proton separation threshold in this nucleus: $S_p = 1773(10)$ keV. This new value is an important ingredient for the determination of the excited states based on the energies of protons emitted from ^{44}V. Indeed, β decay of ^{44}Cr populates proton-unbound states of ^{44}V, one

of which is the 0^+, $T = 2$ IAS of the ^{44}Cr ground state, as shown in Fig. 5. β-delayed proton emission from ^{44}Cr has been observed experimentally [29,30]. No firm assignment of the 0^+, $T = 2$ state exists. Some of the observed peaks could belong to the proton emission from the Gamow-Teller populated 1^+, $T = 1$ states. Future experiments on β-delayed spectroscopy of ^{44}Cr should be able to at least pin down the excited level of the 0^+, $T = 2$ IAS in ^{44}V, and using the new mass value, constrain the mass of ^{44}Cr with greater precision.

V. CONCLUSIONS

The first Penning trap mass measurements of ^{44}V ground and isomeric states were performed. The two states were resolved in the Penning trap, lowering the mass uncertainties of these two states from the values reported previously [31] by a factor of 2-4. This provided a lens to probe the improbable value of the IMME c coefficient for the $A = 44$, $T = 1$ multiplet. The new values of the b and c coefficients extracted for the 2^+ and 6^+ triplets are in good agreement with the known systematics and with the IMME. The experimental MEDs and TEDs also support isospin symmetry the $A = 44$, $T = 1$ triplet. A new value for the proton separation threshold in ^{44}V has been determined to an uncertainty of 10 keV. This should help identify the IAS in future experiments on β-delayed proton spectroscopy of ^{44}Cr. Finally, the mass measurement of ^{44}Cr would provide complete information on the isobaric quintet $(T = 2)$ and check the possibility of expanding the IMME to higher terms.

[1] J. Chadwick, Proc. R. Soc. Lond. A **136**, 692 (1932).

[2] W. Heisenberg, Z. Phys. **77**, 1 (1932).

[3] E. Wigner, in *Proceedings of the Robert A. Welch Foundation Conference 1. Benchmark Papers in Nuclear Physics, Vol. 1: Nuclear Analogue States*, edited by D. Robson and J. Fox (John Wiley & Sons, New York, 1957), pp. 67–91.

[4] Y. H. Lam, B. Blank, N. A. Smirnova, J. B. Bueb, and M. S. Antony, At. Data Nucl. Data Tables **99**, 680 (2013).

[5] M. MacCormick and G. Audi, Nucl. Phys. A **925**, 61 (2014).

[6] J. Jänecke, Nucl. Phys. A **128**, 632 (1969).

[7] G. Bertsch and S. Kahana, Phys. Lett. B **33**, 193 (1970).

[8] W. Benenson and E. Kashy, Rev. Mod. Phys. **51**, 527 (1979).

[9] J. Jänecke, Phys. Rev. **147**, 735 (1966).

[10] W. Ormand and B. Brown, Nucl. Phys. A **491**, 1 (1989).

[11] S. Nakamura, K. Muto, and T. Oda, Nucl. Phys. A **575**, 1 (1994).

[12] M. Bentley and S. Lenzi, Prog. Part. Nucl. Phys. **59**, 497 (2007).

[13] K. Kaneko, T. Mizusaki, Y. Sun, S. Tazaki, and G. de Angelis, Phys. Rev. Lett. **109**, 092504 (2012).

[14] K. Kaneko, Y. Sun, T. Mizusaki, and S. Tazaki, Phys. Rev. Lett. **110**, 172505 (2013).

[15] Y. H. Lam, N. A. Smirnova, and E. Caurier, Phys. Rev. C **87**, 054304 (2013).

[16] O. Klochko and N. A. Smirnova, arXiv:1912.09915 [nucl-th] (2019).

[17] B. A. Brown and B. Wildenthal, Annu. Rev. Nucl. Part. Sci. **38**, 29 (1988).

[18] B. A. Brown and W. A. Richter, Phys. Rev. C **74**, 034315 (2006).

[19] M. Honma, T. Otsuka, B. A. Brown, and T. Mizusaki, Phys. Rev. C **69**, 034335 (2004).

[20] A. Poves, J. Sánchez-Solano, E. Caurier, and F. Nowacki, Nucl. Phys. A **694**, 157 (2001).

[21] W. E. Ormand and B. A. Brown, Phys. Rev. C **52**, 2455 (1995).

[22] W. E. Ormand, B. A. Brown, and M. Hjorth-Jensen, Phys. Rev. C **96**, 024323 (2017).

[23] J. C. Hardy and I. S. Towner, Phys. Rev. C **91**, 025501 (2015).

[24] N. A. Smirnova and L. Xayavong, in *Proceedings of the International Conference 'Nuclear Theory in the Supercomputing Era—2018' (NTSE-2018), Daejeon, South Korea, October 29–November 2, 2018*, edited by A. M. Shirokov and A. I. Mazur (Pacific National University, Khabarovsk, Russia, 2019).

[25] G. Audi, M. Wang, A. Wapstra, F. Kondev, M. MacCormick, X. Xu, and B. Pfeiffer, Chin. Phys. C **36**, 1287 (2012).

[26] G. Audi, F. Kondev, M. Wang, B. Pfeiffer, X. Sun, J. Blachot, and M. MacCormick, Chin. Phys. C **36**, 1157 (2012).

[27] M. J. Taylor, M. A. Bentley, J. R. Brown, P. E. Kent, R. Wadsworth, C. J. Lister, D. Seweryniak, M. P. Carpenter, R. V. F. Janssens, S. Zhu, T. Lauritsen, L.-L. Andersson, E. K. Johansson, P. E. Garrett, K. L. Green, G. A. Demand, and S. M. Lenzi, Phys. Rev. C **84**, 064319 (2011).

[28] M. Wang, G. Audi, F. Kondev, W. Huang, S. Naimi, and X. Xu, Chin. Phys. C **41**, 030003 (2017).

[29] C. Dossat, N. Adimi, F. Aksouh, F. Becker, A. Bey, B. Blank, C. Borcea, R. Borcea, A. Boston, M. Caamano, G. Canchel, M. Chartier, D. Cortina, S. Czajkowski, G. de France, F. de Oliveira Santos, A. Fleury, G. Georgiev, J. Giovinazzo, S. Grévy, R. Grzywacz, M. Hellström, M. Honma, Z. Janas, D. Karamanis, J. Kurcewicz, M. Lewitowicz, M. L. Jiménez, C. Mazzocchi, I. Matea, V. Maslov, P. Mayet, C. Moore, M. Pfützner, M. Pravikoff, M. Stanoiu, I. Stefan, and J. Thomas, Nucl. Phys. A **792**, 18 (2007).

[30] M. Pomorski, M. Pfützner, W. Dominik, R. Grzywacz, A. Stolz, T. Baumann, J. S. Berryman, H. Czyrkowski, R. Dąbrowski, A. Fijałkowska, T. Ginter, J. Johnson, G. Kamiński, N. Larson, S. N. Liddick, M. Madurga, C. Mazzocchi, S. Mianowski, K. Miernik, D. Miller, S. Paulauskas, J. Pereira, K. P. Rykaczewski, and S. Suchyta, Phys. Rev. C **90**, 014311 (2014).

[31] Y. H. Zhang, P. Zhang, X. H. Zhou, M. Wang, Y. A. Litvinov, H. S. Xu, X. Xu, P. Shuai, Y. H. Lam, R. J. Chen, X. L. Yan, T. Bao, X. C. Chen, H. Chen, C. Y. Fu, J. J. He, S. Kubono, D. W. Liu, R. S. Mao, X. W. Ma, M. Z. Sun, X. L. Tu, Y. M.

Xing, Q. Zeng, X. Zhou, W. L. Zhan, S. Litvinov, K. Blaum, G. Audi, T. Uesaka, Y. Yamaguchi, T. Yamaguchi, A. Ozawa, B. H. Sun, Y. Sun, and F. R. Xu, Phys. Rev. C **98**, 014319 (2018).

[32] D. Morrissey, B. Sherrill, M. Steiner, A. Stolz, and I. Wiedenhoever, Nucl. Instrum. Methods Phys. Res. B **204**, 90 (2003).

[33] C. Sumithrarachchi, D. Morrissey, S. Schwarz, K. Lund, G. Bollen, R. Ringle, G. Savard, and A. Villari, Nucl. Instrum. Methods Phys. Res. B **463**, 305 (2020).

[34] R. Ringle, S. Schwarz, and G. Bollen, Int. J. Mass Spectrom. **349–350**, 87 (2013).

[35] S. Schwarz, G. Bollen, R. Ringle, J. Savory, and P. Schury, Nucl. Instrum. Methods Phys. Res. A **816**, 131 (2016).

[36] K. Blaum, D. Beck, G. Bollen, P. Delahaye, C. Guénaut, F. Herfurth, A. Kellerbauer, H.-J. Kluge, D. Lunney, S. Schwarz, L. Schweikhard, and C. Yazidjian, Europhys. Lett. (EPL) **67**, 586 (2004).

[37] A. Kwiatkowski, G. Bollen, M. Redshaw, R. Ringle, and S. Schwarz, Int. J. Mass Spectrom. **379**, 9 (2015).

[38] G. Bollen, R. B. Moore, G. Savard, and H. Stolzenberg, J. Appl. Phys. **68**, 4355 (1990).

[39] M. König, G. Bollen, H.-J. Kluge, T. Otto, and J. Szerypo, Int. J. Mass Spectrom. Ion Processes **142**, 95 (1995).

[40] R. T. Birge, Phys. Rev. **40**, 207 (1932).

[41] R. Ringle, T. Sun, G. Bollen, D. Davies, M. Facina, J. Huikari, E. Kwan, D. J. Morrissey, A. Prinke, J. Savory, P. Schury, S. Schwarz, and C. S. Sumithrarachchi, Phys. Rev. C **75**, 055503 (2007).

[42] A. Kellerbauer, K. Blaum, G. Bollen, F. Herfurth, H.-J. Kluge, M. Kuckein, E. Sauvan, C. Scheidenberger, and L. Schweikhard, Eur. Phys. J. D **22**, 53 (2003).

[43] J. Stadlmann, M. Hausmann, F. Attallah, K. Beckert, P. Beller, F. Bosch, H. Eickhoff, M. Falch, B. Franczak, B. Franzke, H. Geissel, T. Kerscher, O. Klepper, H.-J. Kluge, C. Kozhuharov, Y. Litvinov, K. Löbner, M. Matoš, G. Münzenberg, N. Nankov, F. Nolden, Y. Novikov, T. Ohtsubo, T. Radon, H. Schatz, C. Scheidenberger, M. Steck, H. Weick, and H. Wollnik, Phys. Lett. B **586**, 27 (2004).

[44] A. A. Valverde, M. Brodeur, G. Bollen, M. Eibach, K. Gulyuz, A. Hamaker, C. Izzo, W.-J. Ong, D. Puentes, M. Redshaw, R. Ringle, R. Sandler, S. Schwarz, C. S. Sumithrarachchi, J. Surbrook, A. C. C. Villari, and I. T. Yandow, Phys. Rev. Lett. **120**, 032701 (2018).

[45] B. A. Brown and W. D. M. Rae, Nucl. Data Sheets **120**, 115 (2014).

[46] M. G. van der Merwe, W. A. Richter, and B. A. Brown, Nucl. Phys. A **579**, 173 (1994).

[47] S. M. Lenzi, N. Mărginean, D. R. Napoli, C. A. Ur, A. P. Zuker, G. de Angelis, A. Algora, M. Axiotis, D. Bazzacco, N. Belcari, M. A. Bentley, P. G. Bizzeti, A. Bizzeti-Sona, F. Brandolini, P. von Brentano, D. Bucurescu, J. A. Cameron, C. Chandler, M. De Poli, A. Dewald, H. Eberth, E. Farnea, A. Gadea, J. Garces-Narro, W. Gelletly, H. Grawe, G. Martínez-Pinedo, R. Menegazzo, J. Nyberg, Z. Podolyak, A. Poves, R. V. Ribas, C. Rossi Alvarez, B. Rubio, J. Sánchez-Solano, P. Spolaore, T. Steinhardt, O. Thelen, D. Tonev, A. Vitturi, W. von Oertzen, and M. Weiszflog, Phys. Rev. Lett. **87**, 122501 (2001).

[48] A. P. Zuker, S. M. Lenzi, G. Martínez-Pinedo, and A. Poves, Phys. Rev. Lett. **89**, 142502 (2002).

[49] M. A. Bentley, S. M. Lenzi, S. A. Simpson, and C. A. Diget, Phys. Rev. C **92**, 024310 (2015).

[50] A. Boso, S. M. Lenzi, F. Recchia, J. Bonnard, A. P. Zuker, S. Aydin, M. A. Bentley, B. Cederwall, E. Clement, G. de France, A. Di Nitto, A. Dijon, M. Doncel, F. Ghazi-Moradi, A. Gadea, A. Gottardo, T. Henry, T. Hüyük, G. Jaworski, P. R. John, K. Juhász, I. Kuti, B. Melon, D. Mengoni, C. Michelagnoli, V. Modamio, D. R. Napoli, B. M. Nyakó, J. Nyberg, M. Palacz, J. Timár, and J. J. Valiente-Dobón, Phys. Rev. Lett. **121**, 032502 (2018).

[51] J. R. Grover, Phys. Rev. **157**, 832 (1967).